All-optical Multi-wavelength Virtual Memory Architecture
Design and Performances Analysis

Selma Batti[1], Mourad Zghal[2] and Noureddine Boudriga[1]

[1]*Communication Networks and Security Laboratory (CNAS), Engineering School of Communication of Tunis (Sup'Com),*
University of Carthage, Ariana, Tunisia
[2]*CIRTA'COM Laboratory, Engineering School of Communication of Tunis (Sup'Com), University of Carthage,*
Ariana, Tunisia

Keywords: Optical Buffering, All-optical Memory, Fiber Bragg Grating, Tunable Wavelength Conversion.

Abstract: As all-optical memory represents one of the most important lacks in evolution of optical networks; this paper presents an all-optical virtual memory based on a recirculation loop, with the goal of providing optical data unit storage in all-optical switching networks. The concept of multi-wavelength signal buffering is adopted, to realize a shared buffer with an important storage capacity. We propose the organization of the buffer in two loops, the first as a delay loop and the second as an amplification loop, to improve the buffering duration and performances. The memory implementation is demonstrated using optical components such as fiber Bragg gratings (FBG), circulator and tunable wavelength converter. An all-optical control unit is designed to provide a dynamic and automatic signal buffer managing. An analytical model is implemented and a simulations set is done to prove that the proposed architecture is able to confine several signals for a relatively long time as a memory and signals can leave the architecture for a reasonably short delay after the departure decision is taken. The low penalty observed shows good system reliability.

1 INTRODUCTION

To resolve the increasing need of capacity, networking is interesting more and more in optical technologies. However, the absence of optical memory causes a bottleneck due to the optical-electronic-optical signal conversion. To improve optical network performances, all-optical memory is considered as a crucial point. The design of optical memory has important effect on the development of all-optical network and more especially on optical switching node by reducing the impact of some technical problems such as contention resolution (Mack et al., 2010).

We define all-optical virtual memory as a device able to deliver a signal identical to the received one but after a certain delay. Optical data would be kept in optical format throughout the storage time without being converted into electronic format. The multi-wavelength memory must be able to enclose several signals having different wavelengths values at the same time and each one can be delivered independently of the others. To be considered as acceptable, optical buffers must minimally provide

some criteria (Burmeister et al., 2008), such as being bit rate scalable to greater than 40 Gbits/s, being able to memorize data units having at least 40 bytes as size additional to their guard bands and providing dynamically variable memorization time.

A wide variety of architectures has been proposed in the literature for the design of optical buffer. Two main techniques were developed: fiber delay line (FDL) and recirculation loop. The time buffer described in (LeGrange et al., 2007) is based on FDL. The architecture is proposed particularly to be implemented inside an all-optical router. It utilizes fast wavelength switching in combination with an arrayed waveguide grating (AWG) to select a particular FDL from an array of FDL of varying length. An integrated optical device consisting of the silicon delay line and the gate matrix operating as a buffer at 40 Gbits/s is demonstrated in (Park et al., 2008). Once optical packets are routed into the delay line, they are stored in the delay line until the gate matrix switch re-routes them to the output. The gate matrix switch is controlled by an electronic device. Offering a particular small size and a low cross talk, the chosen components enable a 1.1 ns delay of 40 Gbits/s data packets after one turn.

In this work, we propose an all-optical multi-wavelength virtual memory (MWVM). Using all-optical technologies even for the control part, the virtual memory is designed to confine optical signals without resort to electrical conversion during the stay time in the buffer. The multi-wavelength concept allows the share of the unique buffer resource by several signals. Organizing the memory in two loops by isolating the amplifier in a second loop improves the memory performances through guarantee adequate power level and avoiding additional noise amplification. Moreover, we size the duration of a first loop to reduce the delay between the moment of the exit decision and the signal deliverance and to provide an enough long buffering duration. Work presented in (Batti et al., 2010) describes an all-optical virtual memory allowing the confinement of a single signal. In the new all-optical multi-wavelength virtual memory, several signals having different wavelengths can be buffered at the same time. Each signal is delayed for time duration independently of the other signals delays. The designed control unit provides a dynamic managing of the signal exit without resort to external intervention. Virtual memory physical implementation and optical control part are designed to manage the delay of each signal independently of the other signals. To dimension the proposed virtual memory, three criteria are addressed: first loop size, admitted wavelength number and system bit rate. The architecture performances are evaluated by an analysis study and a set of simulations.

The remainder of this paper is organized as follow: Section 2 is dedicated to the description of the design of the novel all-optical multi-wavelength virtual memory; Section 3 presents the analytical model to evaluate the communication performances; simulation and results are given in Section 4; finally, Section 5 concludes this paper.

2 MWVM ARCHITECTURE

In this section, we describe the new architecture of the all-optical multi-wavelength virtual memory. Signals arriving at the memory entrance have to be delayed by turning in the loop. So, each signal has to perform a number of turn independently of the other signals. The information about the required turn number for each arriving signal is generated by a component upstream from the memory and sent to the memory control unit. The maximum signal number turning in the same time in the virtual memory K represents the memory capacity.

Signals arriving to the input block are considered synchronized. This can be ensured by the insertion of synchronizer (Batti et al., 2009) upstream from the virtual memory. That is why we suppose that the data units have the same size or, at least, have a fixed maximum size equivalent to slot duration (S). The synchronizer is an all-optical device able to align data units on a slot starting indicated by a clock signal.

2.1 Loops Architecture and Functioning

Organized in two loops as illustrated in Figure 1, the virtual memory is used to buffer several signals during different time duration. This memorization is done by enclosing signals in the first loop, named delay loop ($L1$ in Figure 1). When the power of a signal reaches an unacceptable level, it is amplified in the second loop, named amplification loop ($L2$ in Figure 1). Implemented using all-optical components, the virtual memory consists of an optical combiner, an optical fiber, a wavelength converters block, an optical amplifier, three circulators and two FBG arrays.
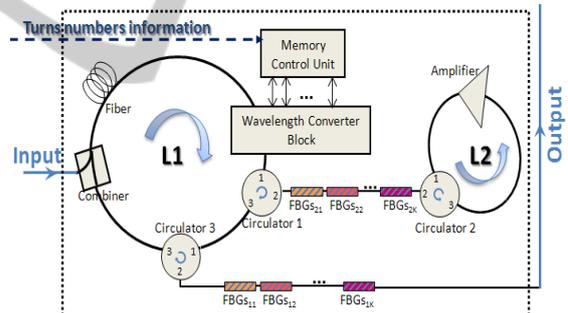
Figure 1: Multi-wavelength virtual memory architecture.

The proposed architecture uses a relatively reduced components number, according to existing architecture. Moreover, the included components are well known devices with reduced complexity functioning. This criterion guarantees that the buffer architecture is implementable.

The fiber inserted in the delay loop has a fixed length L. This length can be assimilated to the first loop length. The second loop encloses only the amplifier, so its length can be considered as quasi null. Each revolution signals are delayed by a time duration ΔT proportional to the fiber length L; this duration is named memory sensitivity. The total delay accumulated by the kth signal after n revolutions in the buffering block is equal to ($n \Delta T$).

The fiber length L must be proportional to the slot duration S, which corresponds to the maximum data unit length, to confine the total signals. The physical implementation of the buffer takes the maximum data unit length into account but remains independent of each data unit length.

An array of FGBs (Srivastava et al., 2008) is inserted at the virtual memory output path and a second array is inserted between the delay loop and the amplification loop. As the buffer can enclose K signals at the same time, each array constitutes a sequence of K reflection bands (RB): the array at the output path constitutes the first sequence of K RB named RB_{k1}, $k \in [0, K[$ and the array between both loops constitutes the second sequence of K RB named RB_{k2}, $k \in [0, K[$. As shown in Figure 2, the RB_{k1} and RB_{k2} are overlapped and the K bands consisting of the union of RB_{k1} and RB_{k2} are disjointed one of the other.
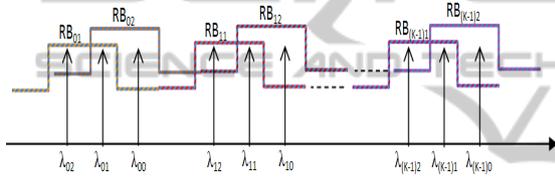
Figure 2: Organization of the reflection bands sequences.

Signals arriving on the input path pass to the delay loop throw the combiner. At this moment, theirs wavelengths are in the band B_1, it means that each kth signal has as wavelength λ_{k1} ($\in RB_{k1} \cap RB_{k2}$), which corresponds to overlapping zone between RB_{k1} and RB_{k2}. Having these wavelengths, signals remain enclosed in the delay loop until theirs wavelengths are converted. Signals pass throw the optical fiber which induces a delay equal to ΔT each revolution. Then, they pass throw the wavelength converter block. The signal number k leaves the converter block with wavelength equal to: λ_{k1} if it has to make another turn in the delay loop, λ_{k2} ($\in RB_{k1}-(RB_{k1} \cap RB_{k2})$) if it has to be amplified and λ_{k0} ($\in RB_{k2}-(RB_{k1} \cap RB_{k2})$) if it has to exit the buffering block. Then, signals reach the first port of the first circulator and they are led to its second port. The signals pass throw the second FBGs array which constitutes the reflection bands RB_{k2}, $k \in [0, K[$. Two cases may occur: signals with wavelengths out of the RB_{k2}, that means signals with wavelengths equal to λ_{k2}, are transmitted to the second circulator; but signals with wavelengths inside the RB_{k2}, that means signals with wavelengths equal to λ_{k1} or λ_{k0}, are reflected to the first circulator. The transmitted signals arrive at the second port of the second circulator and are led to its third port. So these signals enter to the second loop where they are amplified. Passing from the first port to the second port of the second circulator, these signals leave the amplification loop, cross the reflection bands RB_{k2} and are led from the second port to the third port of the first circulator. Also the reflected signals are led from the second port to the third port of the first circulator. Signals arriving at the first port of the third circulator are led to its second port. Then, they pass throw the first FBGs array which constitutes the reflection bands RB_{k1}, $k \in [0, K[$. As happen with the first reflection bands, two cases may occur: signals with wavelengths out of the RB_{k1}, that means signals with wavelengths equal to λ_{k0}, are transmitted on the virtual memory output path; but signals with wavelengths inside the RB_{k1}, meaning signals with wavelengths equal to λ_{k1} or λ_{k2}, $k \in [0, K[$, are reflected to the second port of the third circulator. Transmitted to the third port of the third circulator, the reflected signals reenter to the delay loop and are passed by the combiner to the optical fiber. Signals remain enclosed in the delay loop until the wavelength converter block shifts theirs wavelengths to: (a) λ_{k2} and so they are passed to the amplification loop, or (b) λ_{k0} to be exited from the memory.

2.2 Wavelength Converter Block

A wavelength converter block is inserted inside the delay loop. This block is used to convert the signals wavelengths independently one of each other. In fact, several signals can be enclosed in the virtual memory at the same time (at most, K signals); signals having to be amplified must have theirs wavelengths converted to λ_{k2} ($k \in [0, K[$); signals which were just amplified, during the previous turn, must have theirs wavelengths reconverted to λ_{k1} ($k \in [0, K[$); signals having to exit the virtual memory to the switching block must have theirs wavelengths converted to λ_{k0} ($k \in [0, K[$) and signals having to turn again in the delay loop must have theirs wavelengths maintained to λ_{k1} (no conversions are needed).

As shown in Figure 3, the wavelength converter block consists in a set of K tunable wavelength converter (Wang et al., 2006) managed by a memory control unit. When signals turning in the delay loop arrive at the wavelength converter block, a demultiplexer separates them on K paths. On each path an optical sensor is used to detect the arrival moment of each signal. These sensors inform the memory control unit of the arrival moment of

signals. Each sensor sends an information signal named $sens_k$, where $k \in [0, K[$ is the range of the sensor. The wavelength converters make the needed conversion or still idle according to the decision of the memory control unit. The control unit generates K control signals organized in an array of control wavelength named $\lambda_c [0..K-1]$. Then, the K paths are regrouped by the multiplexer.
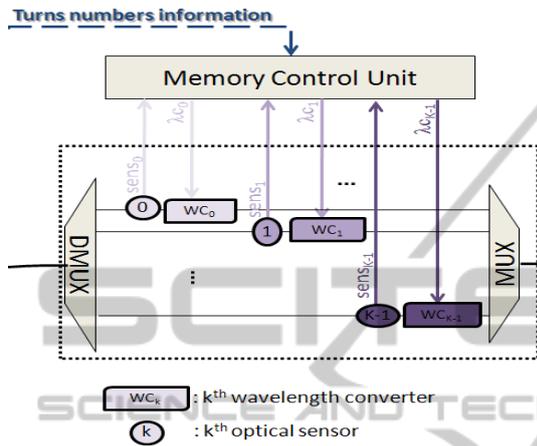
Figure 3: Wavelength converter block architecture.

2.3 Memory Control Unit

The control unit is the component that manages the signals paths by delivering synchronous signals to pilot the wavelength converters. According to the previously received turn number information (sent by a component upstream from the virtual memory), it generates the three kinds of wavelengths summarized in Equation 1 at different moments.

Using all-optical technologies, the control unit consists of three main components as shown in Figure 4: calculator, synchronizer and multi-wavelength sources (MW sources).

The calculator receives the information about required turn numbers for each enclosed signal. According to the physical implementation of the loops, it computes the amplifications number p_k for each signal. Each time a signal crosses the wavelength converter block, the calculator is advertised by the synchronizer and memorizes the turn number for this signal. According to this number, the calculator can let the kth MW source ideal, if no conversions are required; also it can generates a signal indicating to the MW Sources$_k$, $k \in [0, K-1]$, which kind of wavelengths they must generate (λ_{k0}, λ_{k1}, λ_{k2}). So, the calculator has to realize only two simple operations (increment and comparison) which can be carried out in optical

domain.

The synchronizer is used to command the calculator to start the signal generation exactly when the kth signal arrives at the wavelength converter block. In fact, at its arrival, signal crosses the kth optical sensor to inform the control unit of its arrival. If a conversion is required, the control unit must start generating a continuous wave intended for the wavelength converter.

The MW sources are a set of multi-wavelength laser sources generating the wavelengths required to signal conversion. These components receive control signals from the calculator, and generate the optical continuous signals organized in the array of control wavelength $\lambda_c [0..K-1]$. The multi-wavelength laser source can be chosen from the existing components. However, its implementation should pay attention to its response time, since it can affect the system performances.
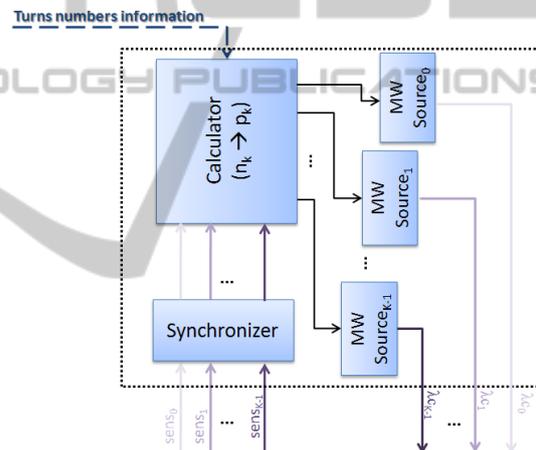
Figure 4: Memory control unit architecture.

Several technologies can be used to provide a wavelength generator for the control unit. Among the most important technologies, one can distinguish two components; the optical flip-flop memory (Kurobe et al., 2007) and the laser neural network (Liu et al., 2004). Due to the described memory control unit, the proposed virtual memory provides a dynamical variable memorization time without resort to electrical domain.

3 PERFORMANCES ANALYSIS

We evaluate performances of the system, and more precisely of the buffering block, by assessing four communication parameters: the delay, the attenuation, the dispersion and the signal to noise

ratio (SNR). In fact, each component crossed by signals adds some delay and signal distortion.

For simplification reasons, we suppose that: (a) the circulator and the combiner have identical effect on signals independently of their input port; (b) all used FBGs have the same effects on the communication performances; (c) the dispersion induced by the cross of the FBGs, the wavelength converter block and the optical amplifier is negligible according to the dispersion induced by the other components; (d) only the optical amplifier and the wavelength converter block in active mode increase the noise.

In this work, n represents the turn number in the delay loop. Each revolution, the crossed components increase the signal distortion by increasing the attenuation, the dispersion and the noise. After a number of turns, the signals power reaches a critical level. That's why amplification must be performed.

After n turns in the memorization loop and p turns in the amplification loop, the kth signal cumulates the total delay given by equation 1, where c, n_{fib} and L are respectively the light celerity, refractive index and fiber length; and the $T_{conv,on}$, $T_{conv,off}$, $T_{FBG,ref}$ and $T_{FBG,trx}$ are respectively the response times of the active wavelength converter, the inactive wavelength converter, the reflecting FBG and the transmitting FBG. One can see that the delay induced by the optical fiber is the most important one according to the delay of the converter and the FBGs. So, the signal rang (k) has a neglected effect on the cumulated delay.

$$
\begin{aligned}
T_{k,n} = & \; n \frac{L \, n_{fib}}{c} + (2n - p - 1) T_{FBG,ref} \\
& + (2p + 1) T_{vonv,on} + (n - 2p - 1) T_{vonv,off} \\
& + [2(k - 1)(2n - p - 1) + K(2p + 1)] T_{FBG,trx} \\
\approx & \; n \frac{L \, n_{fib}}{c}
\end{aligned}
\tag{1}
$$

Equation 2 evaluates the power attenuation occurred to the kth signal after n turns in the memorization loop and p turns in the amplification loop. In this equation, A_{comb}, A_{fib}, A_{cir}, $A_{conv,on}$, $A_{conv,off}$, $A_{FBG,ref}$ and $A_{FBG,trx}$, respectively appoint the attenuation of the combiner, fiber, circulator, wavelength convertor in active mode, wavelength convertor in inactive mode, FBG when signals are reflected and the FBG when signals are transmitted. The G_{amp} is the optical amplifier gain.

$$
\begin{aligned}
A_{k,n} = & \; n \left(A_{comb} + A_{fib} L \right) + (4n + 2p - 1) A_{cir} \\
& + (2p + 1) A_{conv,on} + (n - 2p - 1) A_{conv,off} \\
& + (2n - p - 1) A_{FBG,ref} - p G_{amp} \\
& + [2(k - 1)(2n - p - 1) + K(2p + 1)] A_{FBG,trx}
\end{aligned}
\tag{2}
$$

The accumulated dispersion is given by equation 3 for the kth signal after n turns in the memorization loop and p turns in the amplification loop. The symbols D_{comb}, D_{fib} and D_{cir} give respectively the dispersion of the combiner, fiber and circulator. The $\Delta\lambda$ is the spectral line width of the laser source.

$$
D_{k,n} = n \left(D_{comb} + D_{fib} \, L \, \Delta\lambda \right) + (4n + 2p - 1) D_{cir}
\tag{3}
$$

The equation 4 listed below gives the SNR expression after n turns in the memorization loop, inducing a cascade of p amplifications and $(2p+1)$ wavelength conversions, where P_{in} is the input signal power, $SNR_{conv,on}$ is the SNR introduced by the wavelength converter in active mode, η_{SP} is the ratio of electrons in higher and lower states, h is the Plank's constant, ∇f is the bandwidth that measures the noise figure and G_{amp} is the optical amplifier gain.

$$
SNR_{k,n} = \frac{P_{in} \, SNR_{convon}}{\left[2 p \, \eta_{sp} \, h \, \nabla f \, (G_{amp} - 1) \, \lambda_k \right] SNR_{convon} + (2p + 1) P_{in}}
\tag{4}
$$

4 SIMULATIONS AND RESULTS

4.1 Simulation Model and Parameterization

To demonstrate the proposed memorization function, a multi-wavelength model implemented using the *OptiSystem* simulator and *Matlab* is presented in this section. The laser sources are modeled as pseudo-random bit sequence generators with variable data unit size. Mach-Zehnder modulators are used with continuous wave lasers having a power of 1mW, and NRZ generators. The wavelength converter block is represented by developed Matbab co-simulator components. The FBG arrays are modeled by subsystems of FBGs. The optical receivers are modeled as PIN photodetectors and low pass Bessel filters. The data unit size is fixed to 1500 bytes.

To evaluate the performances limits of the system, we need to implement the worst case, which means, when all the transmitters generate signals having to be enclosed in the buffering block for the maximum time duration.

A set of simulations is performed for several buffering fiber length, capacity and bit rate values. The variations of the delay, attenuation, dispersion and SNR while the turn number is increasing are collected from the list of signal port data of the simulation model layout at the output ports. After

receptions, signals are translated to electrical domain and analyzers show their eye diagram and calculate the maximum Q factor.

4.2 Results Analysis

To evaluate the communication parameters variation in function of the turn number and the signal rank, a first set of simulations is performed where the buffering fiber length is fixed to be equivalent to one data unit size (59,95m), the buffering capacity is equal to four wavelengths and the system bit rate is 40 Gbits/s. The attenuation, the dispersion and the SNR of each signal is depicted while the turn number is increasing.

By examining the curves of Figure 5, one can say that the attenuation depends of the signal rank (k). In fact, as previously illustrated in equation 6, the number of crossed FBG depends of the signal rank. Also, this variation can be explained by the effect of the amplifier on each signal according to its wavelength value.

Figure 6 illustrates the variation of the dispersion while the turn number is increasing for the different signal ranks. It is evident that when turn number increases, the dispersion increases also, as the number of crossed equipments increases. As the fiber, one of most equipment affecting the signal dispersion, adds varied dispersion on signals according to theirs wavelengths, the signal dispersions depend of the signal ranks.

The SNR variation of each signal when turn number is growing is depicted in Figure 7. As each p turns in the first loop, signals have theirs wavelengths converted and are amplified, it is clear that the SNR value decreases. As the amplifier contribution in the SNR depends of the signal wavelength value, curves in Figure 7 are distinguishable.
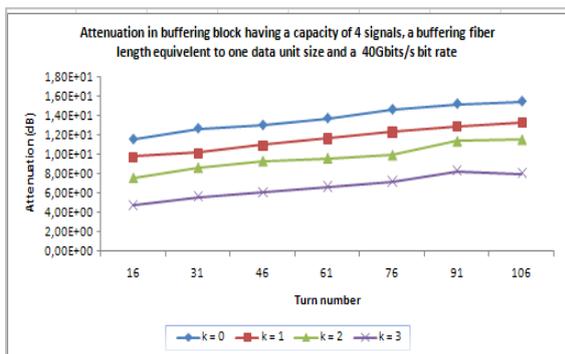
Figure 5: Variation of the attenuation for various turn number and signal ranks.
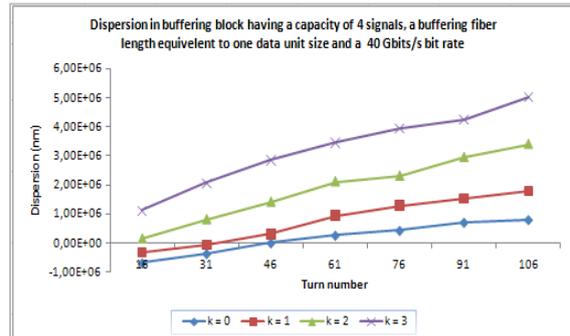
Figure 6: Variation of the dispersion for various turn numbers and signal ranks.
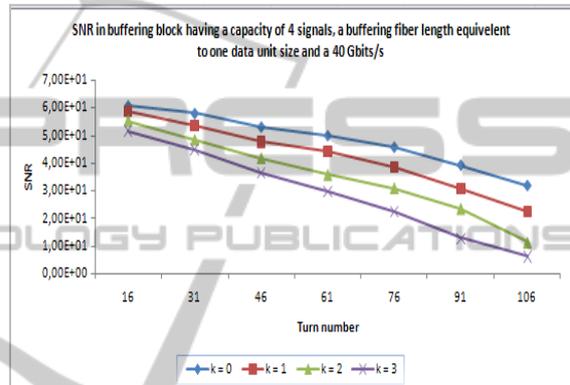
Figure 7: Variation of the SNR for various turn numbers and signal ranks.

To evaluate the effect of the architecture characteristics on signals quality, three simulation sets are performed by fixing two characteristics and varying a third one: the system bit rate, the buffering fiber length and buffering capacity. Firstly, the buffering fiber length and the buffering capacity are fixed respectively to the equivalent one data unit size (1500 bytes) and four wavelengths and the system bit rate is varied to 2,5, 10 and 40 Gbits/s, secondly, the capacity and bit rate are fixed respectively to four wavelengths and 40 Gbits/s and the buffering fiber length is varied to the equivalent of 1, 5 and 10 data unit length, and thirdly, the bit rate and the buffering fiber length are fixed to 40 Gbits/S and the equivalent of one data unit length (59,95 m) and the buffering capacity is varied to one, two, four and height wavelengths. The maximum Q factor is depicted for each signal while the turn number is increasing. Then, the maximum Q factor average is calculated.

In Figure 8, the maximum Q factor average variation for several system bit rates is showed. One can see that the signal quality decreases when the turn number growth. But it remains in acceptable

row for the three bit rates.
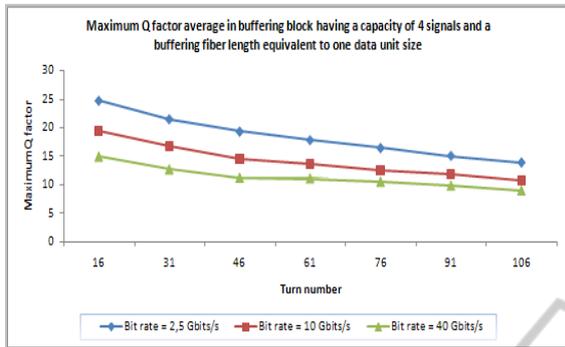
Figure 8: Maximum Q factor average variation for various system bit rates.
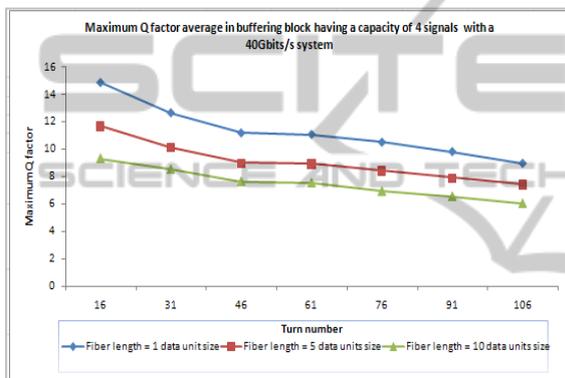
Figure 9: Maximum Q factor average variation for various buffering fiber lengths.

The Maximum Q factor average variation for several buffering fiber lengths is illustrated in Figure 9. While the fiber length (size of the delay loop) is growing, it degrades the signal quality. This fact can be explained by the attenuation and dispersion rising when the crossed fiber length increases.

Figure 10 shows the Maximum Q factor average variation for several buffering capacities. Curves prove that the buffering capacity decreases the signals quality while increasing. This fact can be justified by the crosstalk effect of signals one on another.

Architecture presented in (Park et al., 2008) operates at 40Gbits/s with a single wavelength capacity and 9cm fibre length. After one turn, signal is delayed by 1.1ns with a power penalty of 2.4dB and a Q factor of 6. Authors predict that the architecture is able to achieve 9 or 10 recirculations with the same power penalty. To obtain more delay, using a longer delay line requires the insertion of amplification inside the delay line.

As our architecture includes amplifications only

when needed, in 40Gbits/s system and with four wavelengths capacity, it is able to delay signals for more than 30µs with a Q factor average of 8.
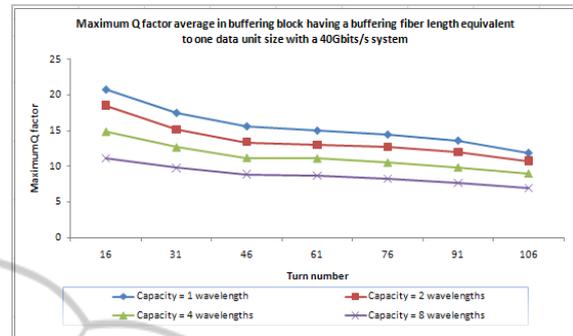
Figure 10: Maximum Q factor average variation for various buffering capacities.

To summarize, one can say that simulations prove that the proposed all-optical multi-wavelength virtual memory is able to memorize several data units having variable sizes in scalable bit rate systems. Due to the simulation limits, no simulations for more than 8 wavelengths as buffering capacity were performed. However, using the aggregation of several virtual memories can provide an important number of memorized signals.

5 CONCLUSIONS

This work presents a novel architecture of an all-optical multi-wavelength virtual memory based on tunable wavelength converter and FBGs. The architecture is organized in two loops: the first loop encloses the signals during the buffering time, and the second one amplifies the signal optical powers just when they reach a critical level. Several signals can be memorized at the same time and the entrance and the exit of each one is managed independently of the others. The proposition includes all-optical control parts making the virtual memory independent of external events. All decisions are made according to required turn number for each signal calculated on the base of previously received information. The feasibility of this proposition is demonstrated by analyzing the performances of the buffering block. This analysis is confirmed by simulation studies. Our architecture can memorize an important number of signals at the same time with a fine response time (sensitivity) quasi equal to the data unit duration ΔT in a system of 40Gbits/s with a relatively acceptable signal distortion.

394

The all-optical multi-wavelength virtual memory can be implemented inside a switching node to be used as a solution to various traffic engineering tasks. Several traffic engineering applications can be addressed in optical burst switching network such as: contention resolution, delay based quality of service (QoS) provision, call admission control and congestion control.

REFERENCES

Batti, S., Zghal, M., Boudriga, N., Hall, T., 2009. An all-optical synchronizer for switching node using single-sideband modulator and fiber Bragg gratings. In *ISCC*, Tunisia, 5-8 July.

Batti, S., Zghal, M., Boudriga, N., 2010. A new all-optical switching node including virtual memory and synchronizer. In *Journal of Networks*, 5(2), pp. 165-179.

Burmeister, E.F., Blumenthal, D.J., Bowers, J.E., 2008. A comparison of optical buffering technologies. In *Optical Switching and Networking*, 5(1), pp. 10-18.

Kurobe, T., Kimoto, T., Muranushi, K., Kagimoto, T., Kagi, N., Kasukawa, A., Wu, J., Otani, E., Arimoto, H., Tsuji, S., 2007. Tunable laser source for fast wavelength switching using a short-cavity DBR laser packaged with wavelength locker. In *National Fiber Optic Engineers Conference*, 25-29 March.

LeGrange, J. D., Bernasconi, P., Simsarian, J. E., Neilson, D. T., Stiliadis, D., Gripp, J., Zirngibl, M., 2007. Demonstration of a time buffer for an all-optical packet router. In *Journal of Optical Networking*, 6(8), pp. 975-983.

Liu, Y., Hill, M.T., Geldenhuys, R., Canbretta, N., de Waardt, H., Khoe, G,D., Dorren, J.S., 2004. Demonstration of a variable optical delay for a recirculating buffer by using all-optical signal processing. In *IEEE Photonics Technology Letters*, 16(7), pp. 1748-1750.

Mack, J.P., Burmeister, E.F., Garcia, J.M., Poulsen, H.N., Biljana Stamenic, Kurczveil, G., Nguyen, K.N., Hollar, K.,Bowers, J.E., Blumenthal, D.J., 2010. Synchronous optical packet buffers. In, *IEEE Journal of Selected Topics in Quantum Electronics*, 16(5), pp. 1413-1421.

Park, H., Mack, J. P., Blumenthal, D. J., Bowers, J. E., 2008. An integrated recirculating optical buffer. In *Optical Express*, 16, pp. 11124-11131.

Srivastava, R., Singh, R. K., Singh, Y. N., 2008. Fiber-optic switch based on fiber Bragg gratings. In *IEEE Photonics Technology Letters*, 20(18), pp. 1581-1583.

Wang, J., Sun, J., Kurz, J. R., Fejer, M. M., 2006. Tunable wavelength conversion of ps-pulses exploiting cascaded sum- and difference frequency generation in a PPLN-fiber ring laser. In *IEEE Photonics Technology Letters*, 18(20), pp. 2093-2095.